Proceedings of ASME Turbo Expo 2011
GT2011
June 6-10, 2011, Vancouver, British Columbia, Canada

GT2011-46604

AN EXPERIMENTAL STUDY OF THERMAL BARRIER COATINGS AND FILM COOLING ON AN INTERNALLY COOLED SIMULATED TURBINE VANE

F. TODD DAVIDSON
The University of Texas at Austin
Austin, Texas USA

JASON E. DEES*
GE Global Research Center
Niskayuna, NY USA

DAVID G. BOGARD
The University of Texas at Austin
Austin, Texas USA

ABSTRACT

This study investigated the interaction of thermal barrier coatings (TBC) and various film cooling configurations to provide a detailed assessment of the thermal protection on a first stage turbine vane. The internally cooled, scaled-up turbine vane used for this study was designed to properly model the conjugate heat transfer effects found in a real engine. The TBC material was selected to properly scale the thicknesses and thermal conductivities of the model to those of the engine. External surface temperatures, TBC-vane interface temperatures and internal temperatures were all measured over a range of internal coolant Reynolds numbers and mainstream turbulence intensities. The blowing ratio of the various film-cooling designs was also varied. The addition of TBC on the vane surface was found to increase the overall effectiveness of the vane surface just downstream of the coolant holes by up to 0.25 when no film cooling was present. The presence of the TBC significantly dampened the variations in overall effectiveness due to changes in blowing ratio which mitigated the detrimental effects of coolant jet separation. It was also discovered that with the presence of TBC standard round holes showed equivalent, if not better, performance when compared to round holes embedded in a shallow transverse trench.

INTRODUCTION

The operating temperature of modern gas turbine engine combustors has increased significantly over the past decades. The motivation of this temperature increase has been to improve engine efficiency and power output as demonstrated by the Brayton Cycle. However, the increase in combustor temperature has lead to modern engines operating at conditions that exceed the material limitations of the engine components. Consequently, multiple cooling and thermal protection techniques are utilized to ensure that engines continue to operate within safety margins. The first of these techniques is to apply a thermal barrier coating (TBC) to the external surface of critical components. TBC materials, such as yttria stabilized zirconia, provide a thin layer of low conducting material to create a large temperature drop between the hot gas path and the component walls. The second technique to thermally protect the engine is to convectively cool internal passages within the engine components with relatively cooler air, or ‘coolant’, bled off of the compressor upstream of the combustor. The final thermal protection technique that is often utilized is film cooling. Film cooling is the method by which the internal coolant is emitted onto the external surfaces of the engine components. This additional layer of relatively cooler fluid allows for a larger temperature drop between the hot gas path and the component surfaces.

Historically, the design process for turbine components has required a simplification of this complicated fluid dynamic and heat transfer problem. This has led to the practice of decoupling the effects of internal cooling from the effects of film cooling with the use of an adiabatic wall condition. It has been argued that this experimental practice still allows for an accurate assessment of the final vane metal temperature by

*Previously at The University of Texas at Austin

describing the boundary conditions for an FEM solver. However, this practice does not account for conjugate heat transfer effects that, as shown by Harrison and Bogard [1] and Dees et al. [2-6], may have noticeable effects on the true boundary conditions that should be used in computational solutions.

Recent advances in computational power have allowed engine designers to begin directly studying the coupled effects of conjugate heat transfer for specific turbine configurations. However, the results generated from most computational methods must first be baselined against experimental data to validate that the code is properly modeling the physics of the design. Consequently, CFD practitioners have had to look for empirical data provided in the open literature to baseline their code. This data is unfortunately very limited and thus the validity of CFD solutions still remains in question.

Hylton et al. [7] provided some of the first work detailing mid-span surface temperature measurements of a radially cooled conducting turbine vane. Due to the novelty of this work and others such as Turner et al. [8] and Hylton et al. [9], it became an important source of data to benchmark computational simulations even though the scope of the data was rather limited.

Albert et al. [10] developed a matched Bi model to simulate the conjugate heat transfer effects of a film cooled blade leading edge with internal impingement cooling. The film cooling configuration had three rows of shaped holes each with a compound angle of 90°. The primary purpose of the study was to compare the difference in observed effectiveness between the matched Bi model and a geometrically identical adiabatic model. It was found that the higher conductivity of the Bi model contributed to a smoothing of the temperature gradients observed on the blade leading edge as compared to the adiabatic results.

Dees et al. [2-6] designed and tested a roughly 12x scale matched Bi model of the C3X vane in order to study the conjugate heat transfer effects of internal convective cooling and external film cooling. The primary purpose of this work was to provide a thorough examination of realistic turbine vane cooling configurations for the purpose of benchmarking future CFD simulations.

Meier and Gupta [11] provided an overview of the evolution of TBC. The primary focus of this study was to emphasize the importance of understanding the cyclic thermal spallation life of different TBC materials and application methodologies. The study also highlighted the benefits of electron beam-physical vapor deposited (EBPVD) coating methods over other application methodologies. According to Meier and Gupta [11], the application of TBC can reduce the external metal temperature of a turbine component by 167°C.

Feuerstein et al. [12] reviewed the benefits and disadvantages of multiple TBC coating methodologies in terms of their thermal protection results and economic demands. Depending on the coating methodology, Feuerstein et al. [12] reported that yttria stabilized zirconia, a typical material used for TBC application, could have a conductivity between $k = 0.83 – 1.71$ W/mK. The higher end of this range was reported to be for the application method of EBPVD which has typical been used in the most advanced engines due to its cyclic durability. EBPVD, however, does require higher capital requirements as compared to other application methods.

Maikell et al [13] expanded on the previous work of Albert et al. [10] by incorporating a thin layer of simulated TBC on the surface of the blade leading edge. The dimensions and properties of the simulated TBC were chosen to properly scale the thickness and conductivity ratios of the vane and TBC materials in an actual engine. As would be expected the TBC contributed significantly to increasing the observed overall effectiveness at the interface of the simulated TBC and leading edge.

Na et al. [14] completed a computational analysis of the effects of conjugate heat transfer with TBC on a flat plate with cylindrical holes. Na et al. showed that the inclusion of TBC reduces the lateral conduction of the surface thus leading to more discrete temperature gradients under the coolant jets. Without TBC, the lateral conduction helps to reduce the temperature of the entrained mainstream gas due to the proximity of the relatively cold vane wall.

Boyle [15] provided a study on the effects of thermal barrier coatings and how they can be used to significantly reduce the NOx production of an engine while maintaining the same turbine inlet temperature. Boyle discussed the fact that by eliminating external film cooling, and relying solely on internal cooling and TBC, the surface boundary layer remains laminar over a larger portion of the vane surface. This benefit is particularly applicable to smaller turbines in which the Reynolds number of the vane passage is lower than that of larger scale engines. Boyle also found that the inclusion of TBC made the vane less sensitive to external heat transfer coefficient conditions.

Sundaram and Thole [16] studied the effects of deposition, hole blockage and TBC spallation on vane endwall film cooling. This study found that spallation near the leading edge row of cooling holes led to a 10% reduction in adiabatic effectiveness levels while spallation within the midpassage gap had minimal effect on the cooling performance.

As previously mentioned, film cooling is also utilized in conjunction with TBC in order to thermally protect the surface of a turbine component. The ideal film cooling geometry is one that emits a uniform layer of coolant across the entire surface of the engine component. This design is described as a 2D slot and has been studied by Blair [17] and Teekaram [18]. Unfortunately, implementation of a 2D slot is not practical on the body of a turbine vane due, primarily, to mechanical strength limitations. Many film cooling designs are thus comprised of discrete coolant holes. As shown by Bogard and Thole [19], the cooling performance of discrete round holes is limited by the fact that at blowing ratios of approximately $M = 0.6$ the core of the coolant jet emitted from the holes begins to rise off of the turbine vane for moderate density ratios. This behavior eventually leads to a significant drop in film cooling performance once the coolant jet becomes completely detached from the vane.

The performance of discrete round holes may be improved by including a diffuser at the exit of the holes. This design, referred to as a shaped hole, decreases the jet momentum allowing for higher blowing ratios to be achieved before separation is observed. Shaped holes also improve performance by encouraging lateral spreading of the coolant jet. Recently, some studies have shown that performance of round holes may be increased significantly by embedding them in a transverse trench [20-22]. This improvement in performance can be attributed to the designs ability to suppress coolant jet separation and promote lateral spreading of the coolant.

The focus of the current study was to complete a thorough assessment of the performance of various film cooling configurations on a matched *Bi* model vane with and without the inclusion of an external layer of TBC. The concept of a matched *Bi* model is to properly scale the conductive and convective resistances to that which is found in a real engine. It should be recognized that the model is designed to match a range of Biot numbers from approximately 0.3 – 0.6 [2] due to variations in the external heat transfer coefficient. The model in this study should provide accurate measurements of the non-dimensional temperature distributions of a real engine since both the *Bi* number range was matched as well as the ratio of the internal and external heat transfer coefficients to that of a real engine. The validity of this method has been supported by the work of Shih et al. [23]. The three film cooling geometries that were tested were 1.) no film cooling, 2.) round holes and 3.) round holes embedded within a transverse trench. The results without TBC were obtained from previous studies by Dees et al. [5] and were used as a basis of comparison to the results obtained herein.

NOMENCLATURE

Bi	=Biot Number, $\frac{h_e t}{k}$
C	= vane chord length = 56.2 cm
C_p	= pressure coefficient, $\frac{p - p_\infty}{\frac{1}{2}\rho U^2}$
d	= film cooling hole diameter = 4.1 mm
D_h	= coolant channel hydraulic diameter
DR	= coolant to mainstream density ratio = ρ_c/ρ_∞
h	= heat transfer coefficient (W/m^2-K)
H	= vane span height = 54.9 cm
HTU	= high freestream turbulence
k	= thermal conductivity (W/m-K)
LTU	= low freestream turbulence
M	= film cooling blowing ratio = $(\rho_c U_c)/(\rho_\infty U_\infty)$
p	= static pressure, pitch
Re	= Reynolds number
s	= streamwise surface distance from stagnation
t	= thickness of vane wall = 1.27 cm
t	= trench depth = 0.23 cm
T	= temperature
Tu	= Turbulence Intensity
U	= flow velocity
x	= streamwise distance from film cooling hole
z	= spanwise distance from bottom of vane

<u>Greek</u>

Λ_f	= Turbulence integral length scale
η	= adiabatic effectiveness = $(T_\infty - T_{aw})/(T_\infty - T_c)$
ϕ	= overall effectiveness = $(T_\infty - T_{w,e})/(T_\infty - T_c)$

<u>Subscripts</u>

aw	= surface of adiabatic wall
c	= coolant at test vane coolant circuit inlet
C	= true chord of airfoil
e	= external
f	= film at film cooling exit
int	= internal coolant
R	= radial channel
w	= outer wall surface
∞	= freestream
U	= u-bend channel

EXPERIMENTAL FACILITIES AND PROCEDURES

The results from this study were obtained at the Turbulence and Turbine Cooling Research Laboratory (TTCRL) at the University of Texas at Austin. The test setup consists of a low speed closed loop wind tunnel driven by a 50 hp variable speed fan with adjustable pitch. One of the corners of this tunnel has been modified to house a simulated three vane, two passage linear cascade with a 12x scale C3X model center vane. This vane was selected as a comparison to previous work completed by Hylton [7]. The outer walls of the test section were adjusted in order to achieve a non-dimensional pressure distribution that matched a previously generated CFD prediction of a real turbine vane cascade. The test section is shown in Figure 1 while the pressure distribution is shown in Figure 2. The measurement of the pressure distribution was obtained in a previous study [2]. The geometric parameters defining the test section and the standard operating conditions are provided in Table 1.

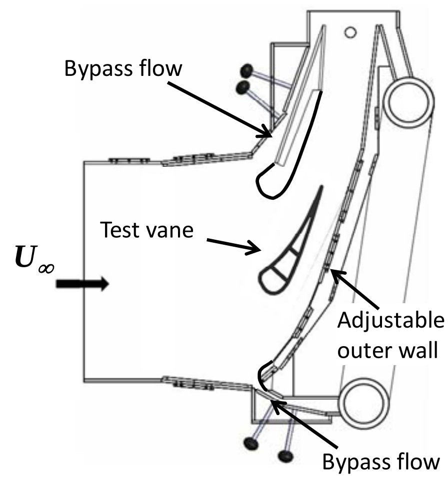

Figure 1: Schematic of turbine vane test section.

A turbulence generator was positioned 0.50 m upstream of the linear cascade in order to obtain the desired mainstream flow conditions. The generator grid consisted of twelve vertical rods 38 mm in diameter spaced 85 mm apart. This grid produced a turbulence level of Tu = 20% and an integral length scale of Λ_f = 3 cm at a location of x/C = 0.26 in front of the leading edge of the simulated turbine vane. These results were obtained with the use of a hot-wire anemometer in a previous study using the same facility [2]. By removing the passive turbulence grid the turbulence intensity decreased to Tu = 0.5% with an integral length scale of Λ_f = 30 cm. These testing conditions are herein referred to as high freestream turbulence (*HTU*) and low freestream turbulence (*LTU*). The *HTU* levels decreased to approximately 5% at the location of coolant injection due to the flow accelerating through the passage.

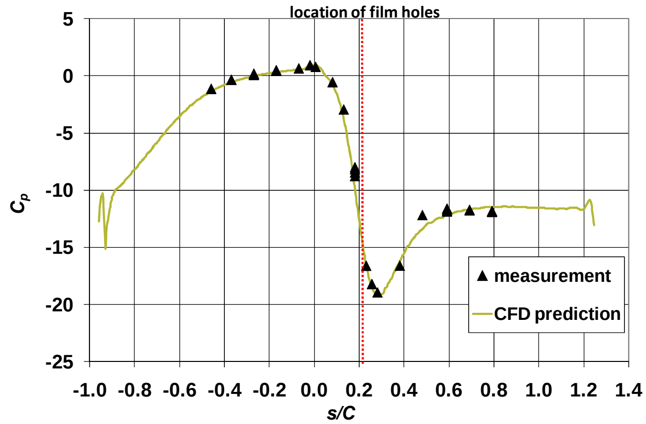

Figure 2: Test airfoil pressure distribution (from [2]).

Table 1: Test section parameters and operating conditions.

Parameter	Value	Units
Chord Length (*C*)	56.2	cm
Vane Span	54.9	cm
Vane Pitch	45.7	cm
Turning Angle	72	degrees
Mainstream Velocity (U_∞)	5.8 ± 0.05	m/s
Mainstream Temperature (T_∞)	305 ± 0.5	K
Density Ratio (*DR*)	1.2 ± 0.1	-
Inlet Reynolds Number	0.75×10^6	-

The coolant was supplied to the vane from a secondary flow loop that was cooled by liquid nitrogen. A diagram of this flow loop is shown in Figure 3. The flow loop draws air off of the mainstream flow downstream of the test section and upstream of the main tunnel fan. The flow is forced through the nitrogen cooled heat exchanger in order to achieve the operating density ratios of *DR* = 1.2. The center test vane consists of a U-bend channel and radial channel to supply internal convective cooling. This design is not an exact replica of a current turbine vane but is realistic none-the-less. Figure 4 provides a schematic of the center test vane. The test vane also has a row of 24 coolant holes on the suction side at a location of s/C = 0.23. These holes were inclined at an angle of 42 degrees with respect to the streamwise direction, had a diameter of 4.1 mm and pitch to diameter spacing of p/d =3. The relative location of the holes may be seen in Figure 5.

The test section of the TTCRL facility was designed in such a manner that allows for the center test vane to be easily removed in order to test alternative vane designs, such as film cooling hole geometry. All of the alternative vane designs retain the same shape factor as the original C3X design in order to ensure that the pressure distribution about the vane remains accurate. Previous studies have completed experiments on both adiabatic and matched *Bi* models with the use of this cartridge system [2-6].

The center test vane was constructed from an epoxy resin with a thermal conductivity of k = 1.02 W/m·K [5]. This material was chosen in order to properly scale the Biot number of the model with that of the engine. As discussed in previous studies [1-6, 23], the purpose of matching the Biot number rather than just the thermal conductivity is to ensure that the ratio of conductive and convective resistances is properly scaled. This ratio may be found in Table 2 along with the associated results for a real engine turbine vane. It is also a necessity to properly match the ratio of the external to internal heat transfer coefficients. This ratio is expected to be between 1 and 10 due to the variations in the local heat transfer coefficient and the internal passage Reynolds number that is selected.

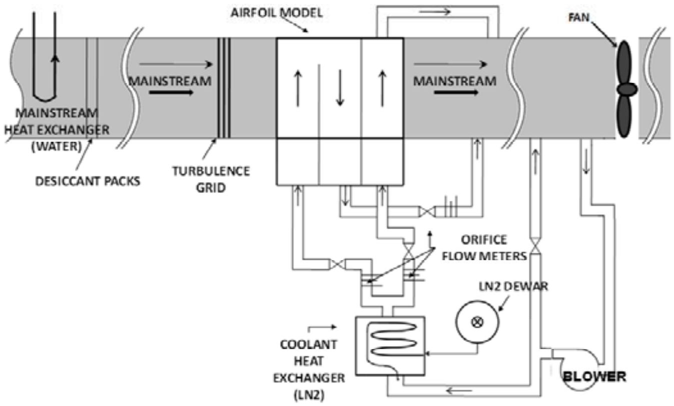

Figure 3: Schematic of secondary flow loop.

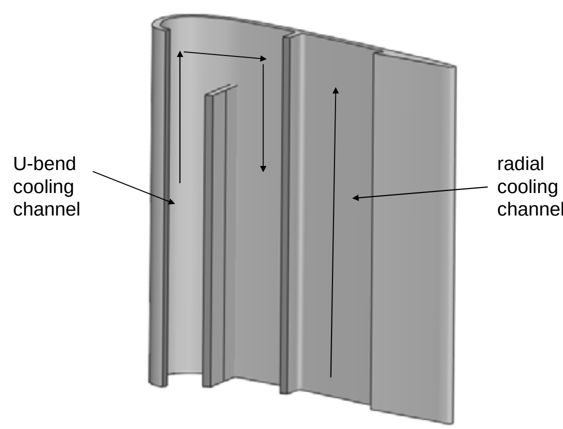

Figure 4: Test airfoil schematic.

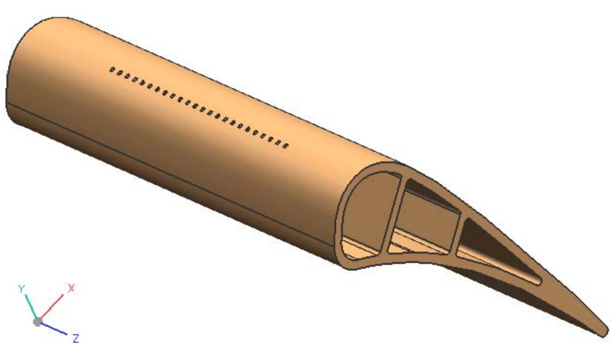

Figure 5: Suction side film cooling holes.

The material chosen for the simulated TBC was cork due to its availability in multiple thicknesses and its flexibility. The conductivity of the cork was independently measured for this study by subjecting the material to a known heat flux and measuring the temperature drop across the material. The combined thermal conductivity of the cork along with a thin adhesive backing was measured to be 0.065 W/m-K. The thickness of the cork and adhesive applied to the surface was l_{cork} = 2.3 mm. This thickness was chosen to properly match the vane to TBC thickness ratio that is found in a real engine. It should be recognized that the thermal resistance of the TBC is approximately three times that of the vane wall. This is important to realize due to the fact that the inclusion of TBC may be expected to have a substantial effect on the thermal behavior of the vane.

A comparison of *Bi* for a real engine versus the model is shown in Table 2. It should be remembered that all of the numbers presented within this table are really more accurately represented by a range of values. Consequently, it is expected that for some design conditions the comparison of *Bi* will be closer and in others it may be further apart.

Table 2: Comparison of vane and TBC material properties.

Parameter	Real Turbine	Model Turbine	Units
Vane Thickness	0.13 – 0.3	1.27	cm
TBC Thickness	0.025 [12]	0.23	cm
Vane Conductivity	20 [13]	1.02 [5]	W/m-K
TBC Conductivity	1.5 [12]	0.065	W/m-K
Heat Transfer Coeff.	1500 - 5000	25 - 90 [2]	W/m^2-K
Vane/TBC Thickness	5.2	5.52	-
Vane/TBC Conductivity	13.3	15.7	-
Vane ***Bi***	0.3 – 0.6 [2]	0.3 – 1.1	-

Prior to testing, the vane was heavily instrumented with surface thermocouples in order to be able to measure the exterior vane wall temperature at the TBC interface. Some of this instrumentation may be seen in Figure 6. If looked at closely, there is a 4 x 3 array of thermocouples just downstream of the suction side row of coolant holes in order to provide greater detail in local temperature measurements. Two of these rows are located at the centerline of separate coolant holes while the other two rows are placed at mid-pitch locations. The three columns of this thermocouple array were placed at locations of approximately x/d = 3, 6, and 15. A line of mid-span thermocouples located at y/H = 0.46 extends from the pressure side location of s/C = -0.82 to the suction side location of s/C = 1.23. The model is also instrumented internally with a similar line of thermocouples at the mid-span location and a more extensive array of instrumentation near the coolant holes.

Once the vane was instrumented, the simulated TBC coating of cork with a thin layer of adhesive tape was applied. The film cooling holes of the vane were plugged with clay in order to allow for baseline testing of the model with no film cooling. Holes were cut in the TBC and the clay plugs were removed to allow for testing with film cooling. Once the cylindrical hole tests were complete, the vane was removed from the test section and the trench was carefully cut into the simulated TBC at right angles. The width of the trench was defined by the breakout area of the embedded holes. This meant that the edges of the trench were immediately adjacent to the edges of the hole. The depth of the trench was defined by the thickness of the TBC that is reported in Table 2. This yields a depth of approximately t/d = 0.56. According to adiabatic studies, the optimal design has a trench wall right next to the breakout of the holes and a depth approaching t/d = 0.75. An optimal trench depth could not be used in this study due to the constraints of matching the thermal resistance of the TBC. However, previous results with trenches show that a design identical to the one presented herein still maintains significantly higher performance over round holes. The resulting round holes and trench configurations are shown in Figure 7.

Figure 6: TBC interface instrumentation.

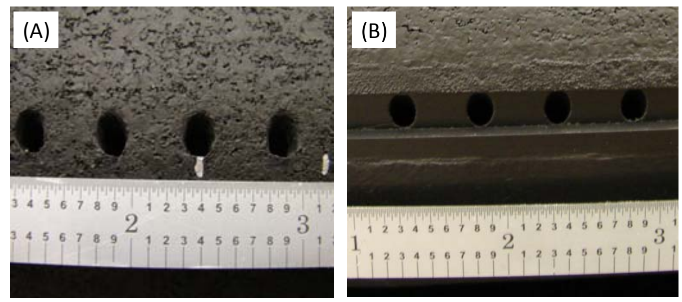

Figure 7: Images of (A) round holes and (B) trench.

Results in this study were obtained for three different film cooling configurations. The configurations are 1.) no film cooling, 2.) round holes, and 3.) round holes embedded in a transverse trench. The film cooling holes for both the round holes and trench configurations were identical in geometry except that the relative hole length was longer for the round hole configuration due to the added thickness of the TBC at the exit of the holes. A summary of the configurations tested in this study is shown in Table 3.

Three internal cooling conditions were investigated in this study. These conditions were dependent on what the Reynolds number, based on the hydraulic diameter D_h, was set at for the u-bend and radial inlet channels. All three of the conditions were measured when film cooling was not present. When film cooling was present, for either the round holes or the trench, the internal cooling was held constant at single Reynolds number condition. Table 4 provides a summary of the internal conditions for all configurations tested.

The majority of the results obtained in this study were done so with the use of E-type thermocouples on the interior wall of the vane and at the interface of the TBC and exterior vane wall. Surface measurements were also obtained with the use of FLIR Systems ThermaCAM® P20 & P25 IR cameras. These cameras have a resolution of 1.5 pixels/mm and a usable field of view of 260x240 pixels. These cameras viewed the surface of the vane through either a NaCl or ZnSe window. The images obtained with the cameras were calibrated with in-test thermocouple readings on the surface of the vane. The E-type thermocouples were made from ribbon (approximately 1.5mm x 1.5mm x 0.1 mm) in order to maximize the measurement accuracy of the local surface temperature while minimizing conduction losses along the lead wires. The calibration thermocouples were placed so as to not interfere with the hydrodynamic behavior of the film coolant while still remaining within the field of view of the cameras. Measurements of the exterior vane wall were obtained solely with the IR cameras when TBC was not being used.

Table 3: Summary of tested configurations.

Configuration	TBC	Low *Tu*	High *Tu*	*M*
No Holes*		x		NA
No Holes	x	x	x	NA
Round*		x		0.64, 0.95, 1.30
Round	x	x	x	0.50, 0.64, 0.95, 1.30
Trench	x	x	x	0.50, 0.64, 0.80, 0.95, 1.30

*Completed by Dees [5]

Table 4: Summary of internal Reynolds number conditions.

Parameter	Re_U=10,000 Re_R=10,000	Re_U=20,000 Re_R=20,000	Re_U=40,000 Re_R=20,000
No Film Cooling	✓	✓	✓
Film Cooling		✓	

The uncertainty of the results obtained within this study was determined with the use of statistical analysis of in-test and test-to-test repeatability. The resulting calculations for 95% confidence interval showed uncertainty values of $\delta\phi$ = ±0.01 for direct thermocouple measurements while previous studies have shown that the uncertainty in IR imaging results for the same facility to be $\delta\phi$ = ±0.02 [5]. One of the primary sources of error in this study was ensuring that steady state had been reached. This was mitigated by directly observing surface temperatures over long durations.

RESULTS

The cooling performance of the vane without film cooling is shown in Figure 8. This figure provides a comparison of the overall effectiveness for varying internal Reynolds number conditions with and without TBC. The non-TBC results were obtained from previous work completed by Dees [5]. As would be expected, the inclusion of TBC on the surface of the vane provides a noticeable increase in the overall effectiveness at the interface of the vane wall and the layer of TBC. Figure 8 highlights 1.) how effective TBC is at thermally protecting the surface of the vane and 2.) how important it is to ensure that the internal Reynolds number is driven as high as possible in order to amply cool the external wall of the vane.

Figure 9 shows the relative augmentation in overall effectiveness that may be attributable to the inclusion of TBC for various internal flow conditions. It appears that for the cases studied the relative effectiveness of TBC increases with increasing internal Reynolds numbers. This may be realized by recognizing that the magnitude of the increase in overall effectiveness in Figure 8 remains at approximately 0.20-0.25 at a location of s/C=0.30 regardless of the internal Reynolds number. This conclusion may be altered if higher internal Reynolds numbers had been achievable.

The effect of mainstream turbulence on a non-film cooled vane with TBC is shown in Figure 10. Increasing the mainstream turbulence from *Tu* = 0.5-20% generated minimal change in the overall effectiveness observed at the external wall of the turbine vane. This conclusion held true regardless of changes to the internal Reynolds number of the vane. However, slightly higher variation is observed in plot (C) adjacent to the stagnation line at *s/C*=0. The magnitude of this variation is less than results previously obtained by Dees [5] in which the vane had no TBC. This would imply that the TBC slightly dampens the heat transfer effects induced by higher freestream turbulence levels.

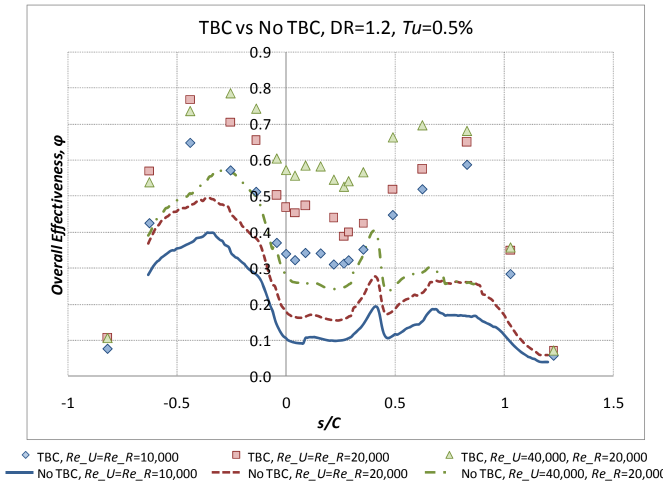

Figure 8: Comparison of external vane wall temperature with and without TBC for varying internal Re.

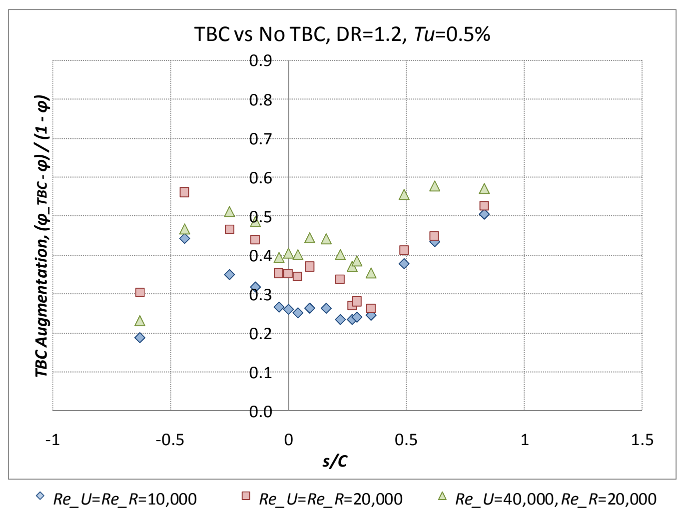

Figure 9: Comparison of TBC augmentation for varying internal Re conditions.

Film cooling results for round holes inclined at 42° at a location of *s/C*=0.23 are shown in Figure 11. The results compare the effects of varying blowing ratio with and without TBC for a constant internal Reynolds number condition. TBC significantly dampens the effect of variations in the film cooling performance due to changes in the blowing ratio, *M*. The general trends still remain in which the overall effectiveness achieved on the external wall begins to decrease as the blowing ratio is increased above *M* = 0.64.

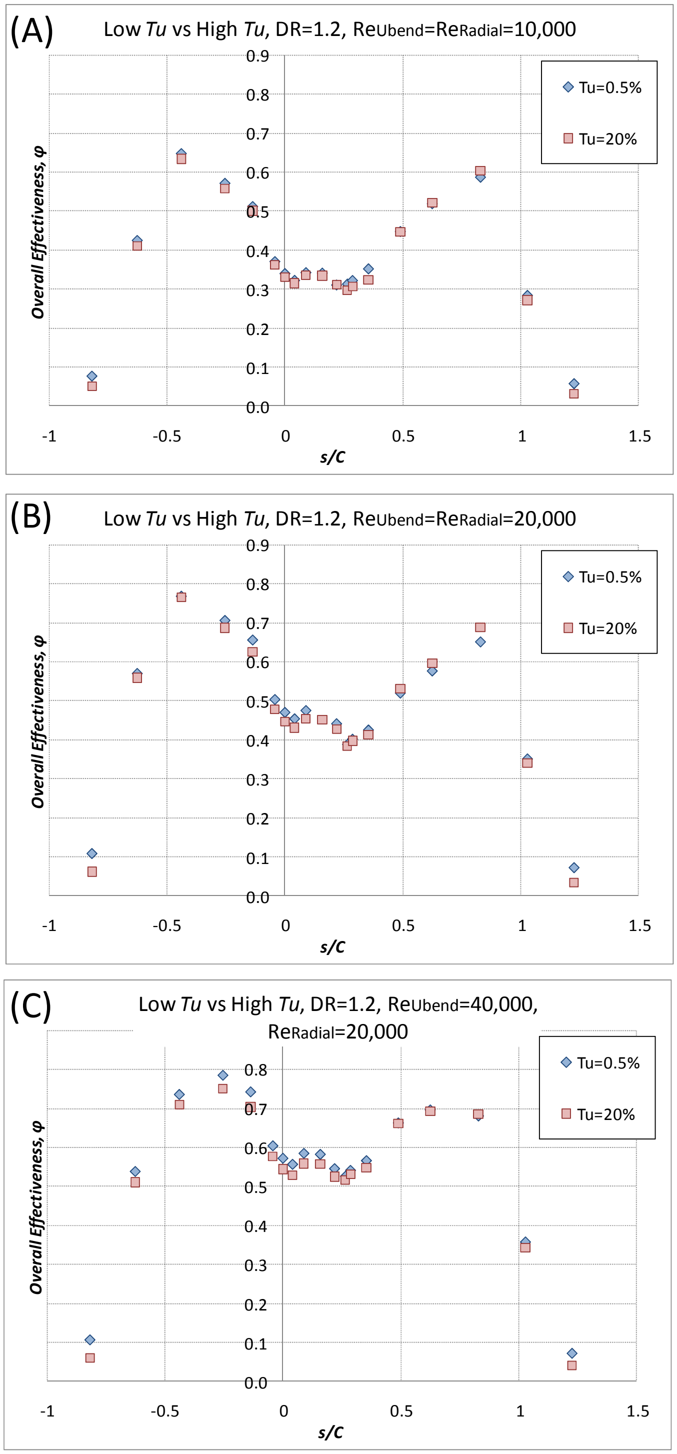

Figure 10: The effect of *Tu* with varying internal Re for a non-film cooled vane with TBC.

Figure 12 provides a further comparison of the effects of film cooling with and without TBC by comparing the performance to the non-film cooled case. It may be recognized that film cooling provides a significant contribution to the overall effectiveness attained at the TBC interface of the vane wall. This contribution is in excess of a 50% improvement just downstream of the coolant holes. This may be due to both the effect of the external film cooling and the convective cooling within the metering holes.

A disagreement may be seen in the data on the pressure side of the airfoil at s/C = -0.13 and -0.25. Initially, one might conclude that this data should be in better agreement since the effect of the film cooling on the suction side should be isolated. This disagreement in the data between the *No Film* and *M*=0.64 cases may be attributed to the fact that there is a higher mass flow rate at the exit of the internal passage for the *No Film* case. This may be explained, in part, by recognizing that the internal Reynolds number for this experimental set-up is defined at the inlet of the vane. When film cooling is present, some of the internal flow is bled off to act as the external film coolant (between 15 – 40% of the air is bled off). This leads to a decrease in the mass flow rate at the exit of the internal passage. The resulting effect may be seen in Figure 12 in which the *No Film* case provides greater cooling on the pressure side due to a higher internal Reynolds number.

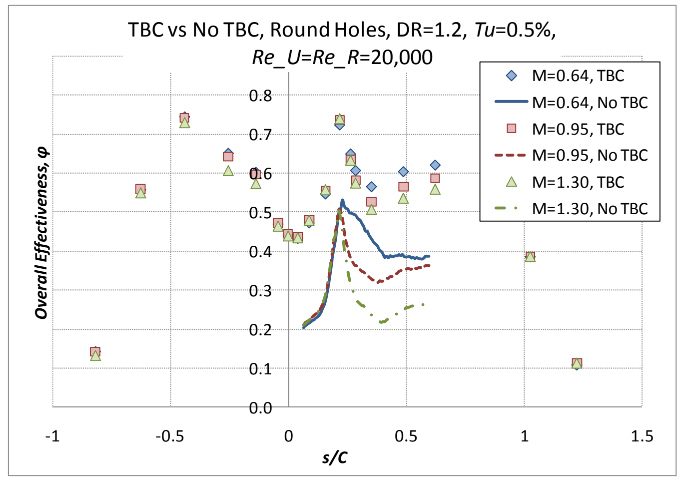

Figure 11: Comparison of round hole film cooling with and without TBC.

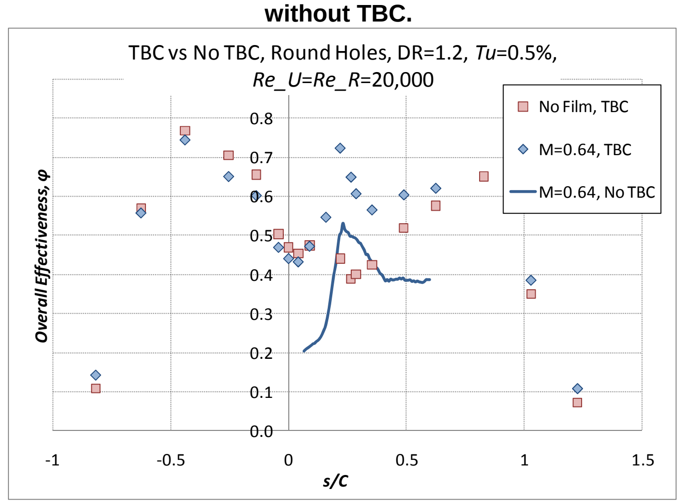

Figure 12: Comparison of TBC effect with and without film cooling.

The effects of variations in mainstream turbulence when round hole film cooling is utilized are shown in Figure 13. This plot shows that at most there is a decrease of 0.05 in overall effectiveness at the interface of the TBC and vane wall due to an increase in the mainstream turbulence from *Tu* = 0.5% to 20%. The magnitude of this effect appears to vary depending on the location on the vane and proximity to the cooling holes. The results of mainstream turbulence effects showed essentially no variability with blowing ratio and thus only a single blowing ratio is presented here.

Figure 14 provides greater insight into the heat transfer behavior of the vane with TBC. This figure provides a comparison of the internal vane wall temperature and the TBC interface temperature. These results were obtained with round hole film cooling at a blowing ratio of M = 0.64 and a high mainstream turbulence level of Tu = 20%. A couple of items are of particular interest. The first is that the largest temperature differentials between the interface and the internal wall are observed near the stagnation region. The second point of interest is that it appears that the temperature differential just downstream of the coolant holes has nearly collapsed.

Multiple internal temperature values are shown in Figure 14 for a single value of s/C ~ 0.28. This is due to the fact that there are multiple spanwise thermocouples at this location. There are also multiple thermocouples in this region for the interface but the data has been averaged to provide an assessment of the laterally averaged performance of the cooling design. Unless otherwise specified, all interface data immediately downstream of the coolant holes has been laterally averaged.

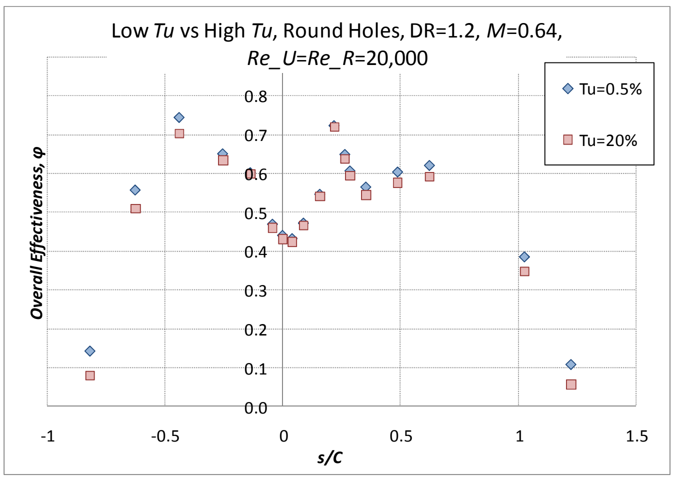

Figure 13: The effect of *Tu* for a round hole film cooled vane with TBC.

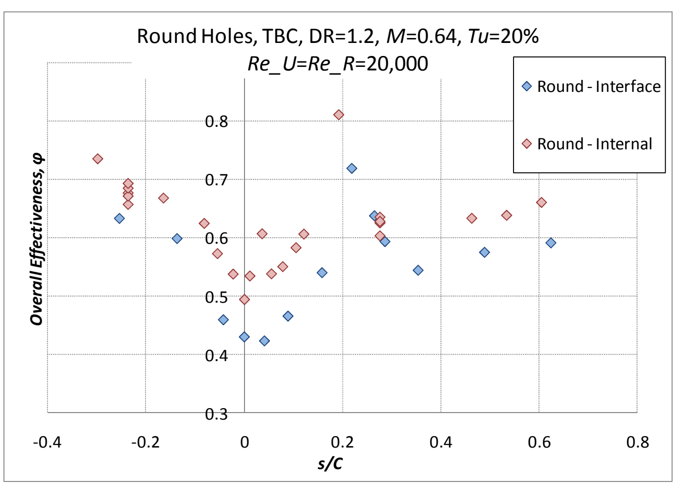

Figure 14: Comparison of vane wall internal and interface temperatures for *M*=0.64 and *HTU*.

Round holes embedded within a transverse trench were examined with particular interest during this study due to the promising results that this design has shown historically in terms of adiabatic effectiveness. Figure 15 below shows a comparison of the trench design to round holes. It may be immediately noticed that the trench design does not appear to improve the overall effectiveness of the vane wall at the TBC

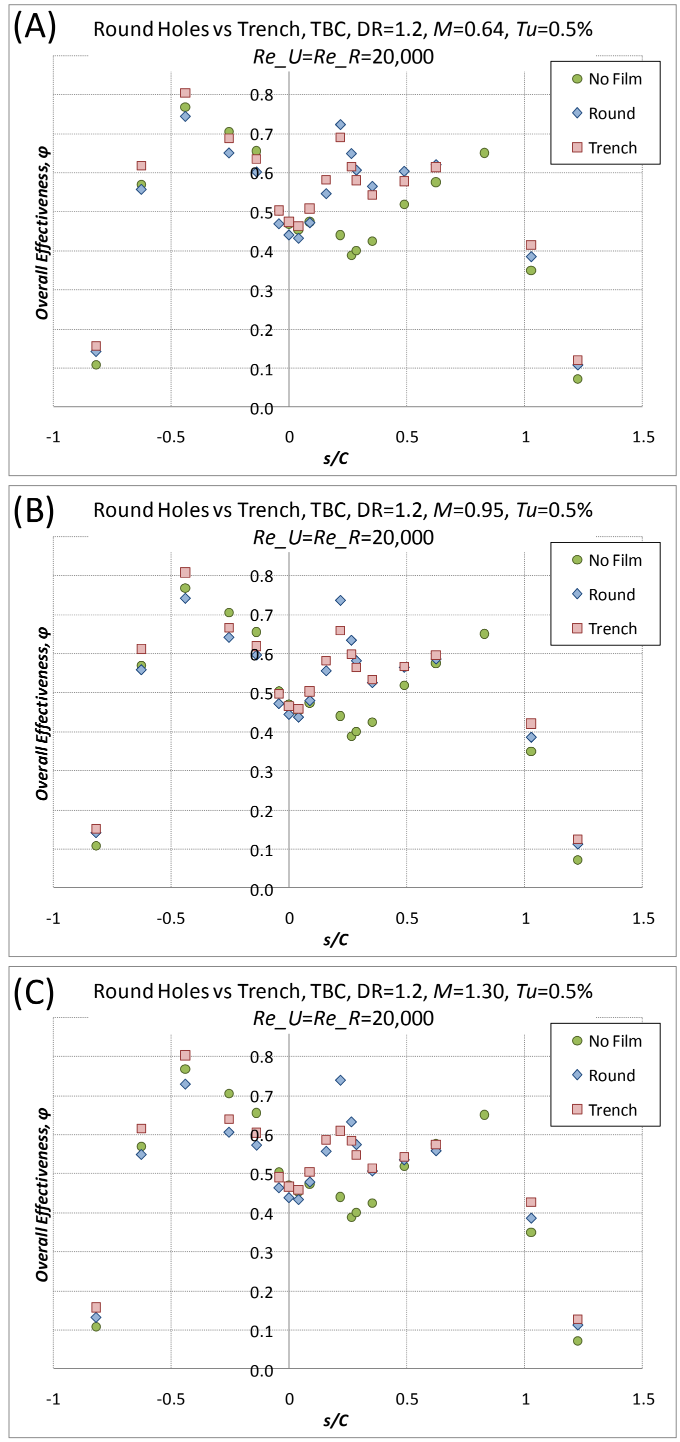

Figure 15: Comparison of round hole and trench film cooling with TBC at *LTU*.

interface regardless of the blowing ratio used. This insensitivity to blowing ratio is of particular interest due to the fact that one of the appealing aspects of the trench design is that it mitigates separation of coolant jets at higher operating blowing ratios. This behavior allows the trench to achieve noticeably higher peak adiabatic effectiveness levels as compared to round holes. However, this characteristic of the trench does not appear to be improving the cooling performance at the TBC interface of a matched *Bi* model vane. It is currently unclear as to exactly why this is the case. However, it may be possible that the presence of the trench increases the local heat transfer coefficient enough to offset the benefits that it has previously shown. It is also possible that by removing the TBC to create the trench structure it has exposed the vane wall to the hot mainstream flow. This could lead to localized heating of the vane wall that could offset some of the hydrodynamic benefits of the trench design.

It should also be recognized that the round holes for this study were fabricated by hand and consequently each had its own unique behavior. Imaging the entire row of holes with an IR camera showed that, in general, the holes all operated in a very similar manner. It is however possible that in shaping the holes by hand that a slight diffuser was created at the exit of the holes. This may cause the round holes to operate at slightly higher performance levels than would be otherwise expected from machined holes. This characteristic seems unlikely when looking at the image in Figure 7.

It should be noted that the authors recognize the peculiarity of the data on the pressure side not coinciding for the round holes and trench configurations. However, the variation between the film cooling configurations and the non-film cooled data on the pressure side may be explained by earlier discussions of how the non-film cooled case will have a slightly higher Reynolds number at the exit of the internal passage. Multiple checks were completed to ensure that the data that is presented herein was steady state, repeatable and consistent. Consequently, there is currently not a specific explanation that would describe why the discrepancy exists between the round holes and trench configuration. Further study and testing would have to be completed to understand the physical mechanism causing the observed thermal behavior.

Figure 16 shows the results for the round holes compared to the trench design for varying blowing ratios at the high turbulence level of Tu = 20%. The results show that in a similar manner as the low turbulence case the round holes appear to be superior to the trench over a large range of blowing ratio conditions. It is possible that this is attributable to some of the previous reasons posed for why the trench might increase the localized heating of the turbine vane wall.

Figure 17 provides a comparison of the measured TBC interface temperature for the trench with varying mainstream turbulence intensities. Only a single blowing ratio of M = 0.64 is presented here due to the consistency of the behavior for the other blowing ratios. It is evident in this figure that increasing the mainstream turbulence does appear to have a slight effect on the cooling performance of the vane. However, the magnitude of this increase does not appear to be equivalent to previously obtained results that did not have TBC present [5].

Figure 18 highlights the differences in observed performance between the round holes and the trench design. This figure presents laterally averaged effectiveness results just downstream of the coolant hole breakout location. Results in terms of the minimum effectiveness measured are also shown. It is important to recognize that the minimum effectiveness is representative of the highest localized temperature that the external vane wall is subject to for the specific design. Understanding the magnitude of this temperature will help constrain the design requirements of the turbine component materials. The results in Figure 18 reinforce the previously asserted idea that the trench underperforms the round holes. Previous work with the trench

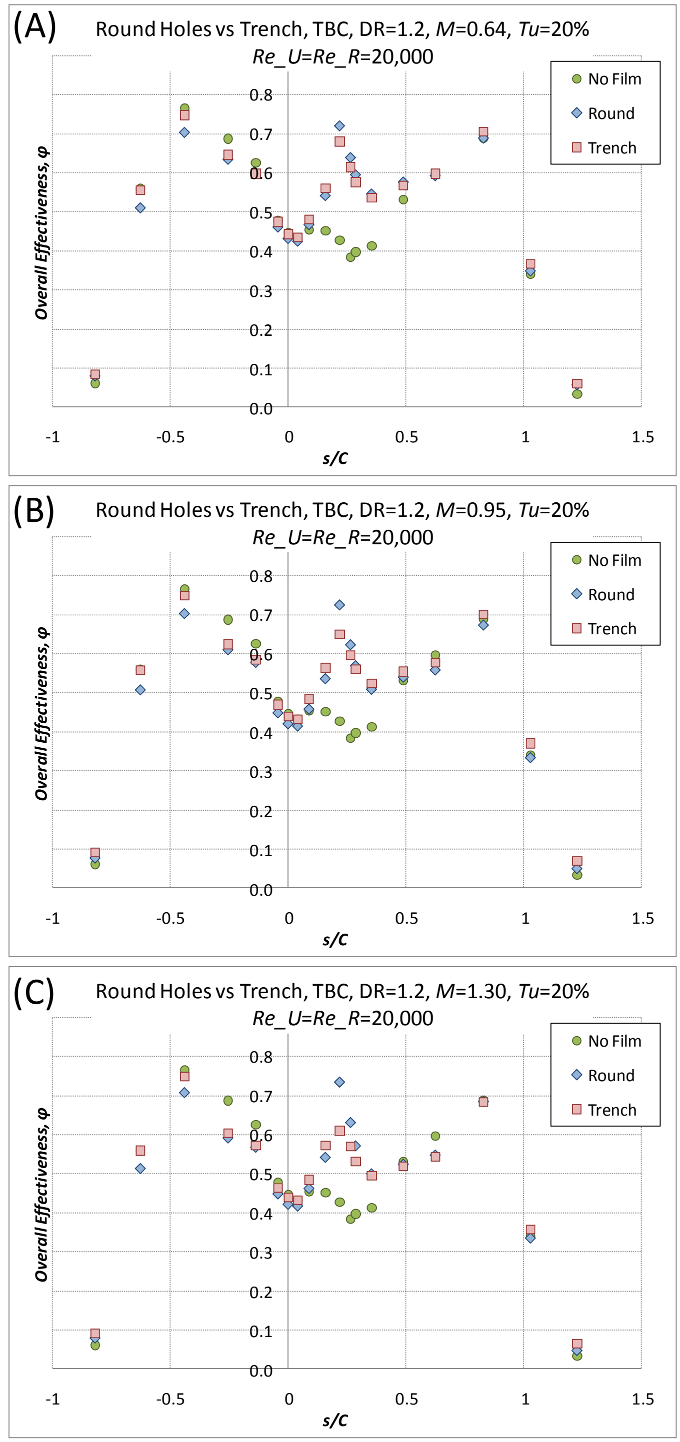

Figure 16: Comparison of round hole and trench film cooling with TBC at *HTU*.

design showed that it promoted significant lateral spreading and smoothing out of the temperature gradients present on the vane surface. It was originally thought that this characteristic might allow the trench to have a relatively uniform lateral temperature profile thus mitigating the negative effects of having localized regions of lower overall effectiveness. However, this is not the case. A closer look at the external surface temperature distribution of the TBC may provide a better understanding of why the trench does not outperform the round holes.

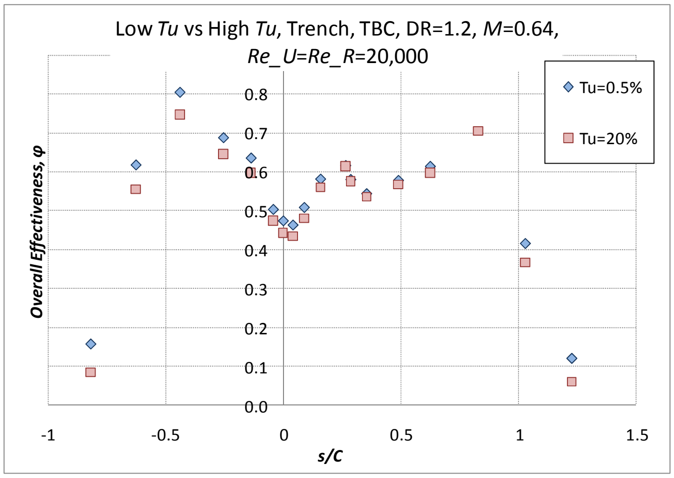

Figure 17: The effect of *Tu* for a trench film cooled vane with TBC.

Looking at Figure 19, one can see how the trench provides significant lateral spreading of the coolant as compared to the discrete nature of the coolant jets from the round holes. This is similar to the previously obtained adiabatic effectiveness results that led to so much interest being directed towards the transverse trench with embedded cylindrical holes [20 – 22]. However, due to the fact that the TBC interface temperature of the trench is not superior to the that of the round holes, it is evident that the trench must increase the localized heating of the vane in another manner. This would imply that the cause for performance degradation is either an increase in local heat transfer coefficient or increased heating due to the exposure of the vane wall within the trench. It is possible that it is a combination of these two.

It is of interest to note that the non-film cooled case appears to have localized cooling just downstream of the plugged coolant holes. Figure 20 shows the effectiveness behavior of a non-filmed cooled vane that is identical to plot (A) in Figure 19 except that it is without TBC. It may be observed that the heat transfer coefficient begins to fall off at approximately s/C = 0.20 before bottoming near s/C = 0.4. The decrease in h may be attributable to the growth of a laminar boundary layer, while the sudden increase in h at s/C = 0.4 was due to boundary layer transition at this point. The decrease in local heat transfer coefficient would lead to lower heat flux to the surface of the vane and thus higher observed cooling performance. This fact may explain why the localized cooling is observed in Figure 19(A). Furthermore, this may imply that the inclusion of TBC on the surface of the vane has done little to alter the boundary layer transition characteristics.

The trench design was further studied by testing at a blowing ratio of M = 0.80. The intention of this was to ensure that a more optimal blowing ratio for the trench had not been missed. The results at a blowing ratio of M = 0.80 showed no improved performance over the previously obtained results at a blowing ratio of M = 0.64. It is believed that a more optimal blowing ratio cannot be found for the current trench design that would allow it to operate at a higher level of performance as compared to the round holes with TBC.

It's possible that if the design of the trench were optimized that it may show improved performance over that of the round holes. The wall height of the current trench design is not the optimal for the inclination angle of the embedded holes. Consequently, the coolant does not impinge on the trench wall in as significant of a manner as it would if the wall height were increased. This leads to decreased lateral spreading of the coolant within the trench before it spills over the wall and coats the TBC surface downstream.

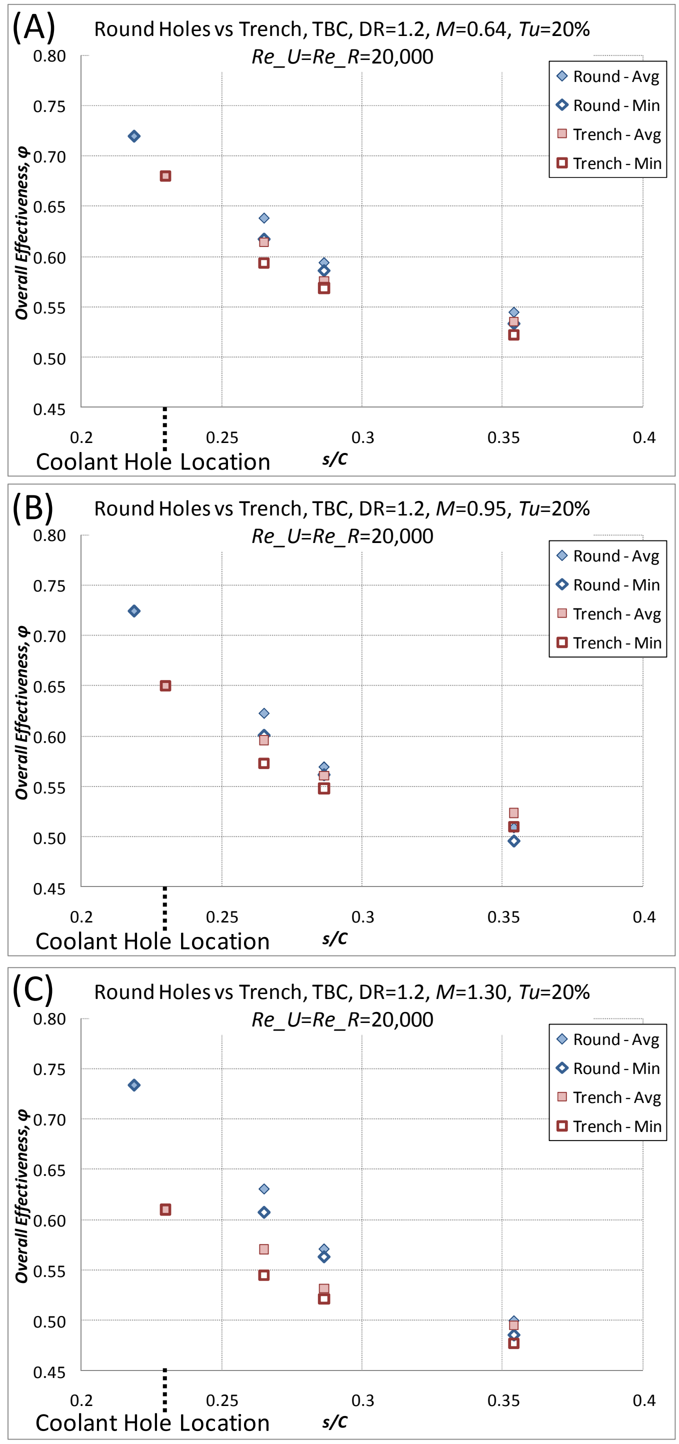

Figure 18: Detailed comparison of round hole and trench film cooling with TBC at *HTU*.

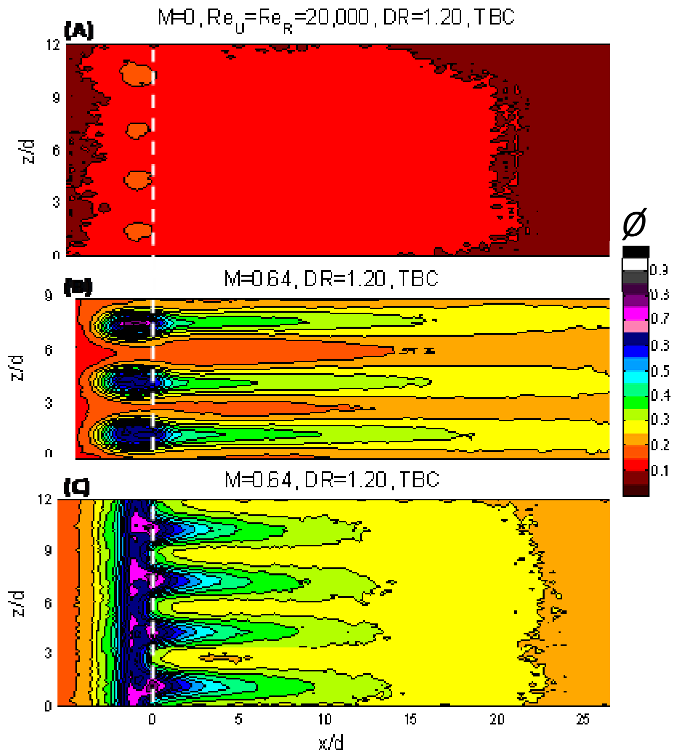

Figure 19: Contour plot comparison of a non-film cooled case with round hole and trench film cooling, all with TBC.

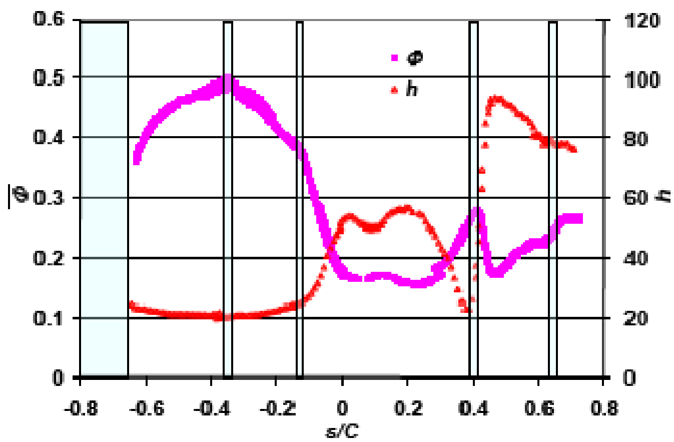

Figure 20: Laterally averaged external *Ø* and *h* for a non-film cooled vane without TBC (*LTU*, *Re$_U$*=20,000) [2].

CONCLUSIONS

In this study an accurate simulation of the effects of TBC on a simulated turbine vane was obtained by designing a large scale vane model for which the Biot number for the vane body and the TBC matched typical engine conditions. By matching the Biot number, the thermal conduction through the vane wall and through the TBC was correctly modeled. The thermal resistance due to the TBC was about three times the thermal resistance of the wall of the model vane, which matched the conditions found for actual turbine hardware. Experiments were conducted to determine how the TBC improved overall cooling effectiveness for a non-film-cooled vane and a film cooled vane using both conventional round holes and a shallow trench configuration.

With no film cooling the TBC was found to increase the overall effectiveness by as much as 200%, i.e. ϕ = 0.1 was increased to ϕ = 0.3. There was a smaller percentage increase with increasing internal coolant flow rates. This increase was expected because the TBC significantly increases the overall thermal resistance for heat flow through the vane. No significant change in overall effectiveness was measured when mainstream turbulence levels were increased from *Tu* = 0.5% to 20%. This is in contrast to decreases in overall effectiveness with increases in mainstream turbulence that were previously measured with no TBC. Apparently the TBC isolates the internal surface of the vane body to an extent that the effects of changing mainstream turbulence are made negligible.

Measurements of the overall effectiveness for film cooling with round holes using a range of blowing ratios showed that the addition of TBC increased overall effectiveness significantly. For example, at optimum blowing ratios where the no TBC case had an overall effectiveness of ϕ = 0.4, addition of TBC increased overall effectiveness to ϕ = 0.6. The percentage increase was greater for higher blowing ratios which had lower overall effectiveness. Variations in the blowing ratio were found to have minimal effect on the overall effectiveness of the turbine vane with TBC. This is in contrast to the conclusion that is often drawn from adiabatic studies.

One of the more interesting results from this study was that a trench formed by the TBC provided no improvement in performance. This was surprising because previous studies of the trench performance in terms of adiabatic effectiveness showed that the trench would generally significantly increase adiabatic effectiveness. Examination of the surface temperatures on the external surface of the TBC showed that the trench did decrease the average temperature of the external surface of the TBC more than the round holes, as expected. Consequently, the lack of improvement in overall effectiveness when using a trench and TBC might be due to increases in heat transfer coefficients caused by the trench and/or heating of the main body of the vane that was exposed within the trench. It is possible that with a more optimal design the trench could achieve higher performance levels.

ACKNOWLEDGEMENTS

The authors gratefully acknowledge the support of the NASA NRA program for this research, and the guidance provided by the Technical Monitor Dr. J. Heidmann. The authors would also like to thank to Office of Naval Research for partial funding of this research through the ESRDC (Electric Ship Research and Development Consortium).

REFERENCES

[1] Harrison, K.L., and Bogard, D.G., 2008, "Use of the Adiabatic Wall Temperature in Film Cooling to Predict Wall Heat Flux and Temperature," ASME paper GT2008-51424.

[2] Dees, J.E., Ledezma, G.A., Bogard, D.G., Laskowski, G.M., Tolpadi, A.K., 2009, "Experimental Measurements and Computational Predictions for an Internally Cooled Simulated Turbine Vane," ASME paper IMECE2009-11622.

[3] Dees, J.E., Ledezma, G.A., Bogard, D.G., Laskowski, G.M., Tolpadi, A.K., 2010, "Experimental and Computational Measurements for an Internally Cooled Simulated Gas Turbine Vane with 90 degree Rib Turbulators," ASME paper GT2010-23004.

[4] Dees, J.E., Ledezma, G.A., Bogard, D.G., Laskowski, G.M., Tolpadi, A.K., 2010, "Momentum and Thermal Boundary Layer Development on an Internally Cooled Turbine Vane," ASME paper GT2010-23008.
[5] Dees, J.E., Ledezma, G.A., Bogard, D.G., Laskowski, G.M., 2011, "Overall and Adiabatic Effectiveness Values on a Scaled Up, Simulated Gas Turbine Vane: Part I – Experimental Measurements", ASME paper GT2011-46612.
[6] Dees, J.E., Ledezma, G.A., Bogard, D.G., Laskowski, G.M., "The Effects of Conjugate Heat Transfer on The Thermal Field Above a Film Cooled Wall: Part I – Experimental Measurements", ASME paper GT2011-46617.
[7] Hylton, L.D., Milhec, M.S., Turner, E.R., Nealy, D.A., and York, R.E., 1983, "Analytical and Experimental Evaluation of the Heat Transfer Distribution Over the Surface of Turbine Vanes," NASA CR 168015.
[8] Turner, E.R., Wilson, M.D., Hylton, L.D., and Kaufman, R.M., 1985, "Analytical and Experimental Heat Transfer Distributions with Leading Edge Showerhead Film Cooling," NASA CR 174827.
[9] Hylton, L.D., Nirmalan, V., Sultanian, B.K., and Kaufman, R.M., 1988, "The Effects of Leading Edge and Downstream Film Cooling on Turbine Vane Heat Transfer," NASA CR 182133.
[10] Albert, J.E., Bogard, D.G., and Cunha, F., 2004, "Adiabatic and Overall Effectiveness for a Film Cooled Blade," ASME Paper GT2004-53998.
[11] Meier, S.M., Gupta, D.K., 1994, "The Evolution of Thermal Barrier Coatings in Gas Turbine Engine Applications", *Journal of Engineering for Gas Turbines and Power*, Vol. 116, pp. 250 – 257.
[12] Feuerstein, A. et al., 2008, "Technical and Economical Aspects of Current Thermal Barrier Coating Systems for Gas Turbine Engines by Thermal Spray and EBPVD: A Review", *Journal of Thermal Spray Technology*, Vol. 17(2), pp. 199-213.
[13] Maikell, J., Bogard, D., Piggush, J., Kohli, A., 2009, "Experimental Simulation of a Film Cooled Turbine Blade Leading Edge Including Thermal Barrier Coating Effects", Paper No. GT2009-60286, ASME Turbo Expo, Orlando, Florida, USA.
[14] Na, S., Williams, B., Dennis, R.A., Bryden, K.M., Shih, T.I-P., "Internal and Film Cooling of a Flat Plate with Conjugate Heat Transfer", Paper No. GT2007-27599, ASME Turbo Expo, Montreal, Canada.
[15] Boyle, R.J., 2006, "Effects of Thermal Barrier Coating on Approaches to Turbine Blade Cooling", Paper No. GT2006-91202, ASME Turbo Expo, Barcelona, Spain.
[16] Sundaram, N., Thole, K.A., 2007, "Effects of Surface Deposition, Hole Blockage, and Thermal Barrier Coating Spallation on Vane Endwall Film Cooling", *Journal of Turbomachinery*, Vol. 129, pp. 599-607.
[17] Blair, M.F., "An Experimental Study of Heat Transfer and Film Cooling on Large-Scale Turbine Endwalls", *Journal of Heat Transfer*, Nov. 1974, pp. 524-529.
[18] Teekaram, A., Forth, C., Jones, T., "Film Cooling in the Presence of Mainstream Pressure Gradients", *Journal of Turbomachinery*, Vol. 113, 1991, pp. 484-492
[19] Bogard, D.G., Thole, K.A., "Gas Turbine Film Cooling", *Journal of Propulsion and Power*, Vol. 22, 2006, pp. 249-270.
[20]Bunker, R., 2002, "Film Cooling Effectiveness due to Discrete Holes Within a Transverse Surface Slot", Paper No. GT-2002-30178, IGTI Turbo Expo, Amsterdam, Netherlands.
[21] Waye, S.K., Bogard, D.G., 2006, "High Resolution Film Cooling Effectiveness Measurements of Axial Holes Embedded in a Transverse Trench with Various Trench Configurations", Paper No. GT-2006-90226, IGTI Turbo Expo, Barcelona, Spain.
[22] Dorrington, J.R., Bogard, D.G., Bunker, R.S., "Film Effectiveness Performance for Coolant Holes Embedded in Various Shallow Trench and Crater Depressions", ASME Paper No. GT2007-27992.
[23] Shih, T., Chi, K., Ramachandran, P., Ames, R., Dennis, R., "The Role of the Biot Number in Turbine-Cooling Design and Analysis", 2010 UTSR Workshop, Oct. 2010.

